Journal of Cleaner Production 165 (2017) 762–776

Contents lists available at ScienceDirect

Journal of Cleaner Production

journal homepage: www.elsevier.com/locate/jclepro

Reducing the environmental impacts of vitreous optical fiber production – A Life Cycle Impact Assessment

Julian T.M. Pinto [a, b, c, *], Karen J. Amaral [d], Susanne Hartard [c], Paulo R. Janissek [e], Klaus Helling [c]

[a] European Commission's Horizon 2020 Programme, AdaptEconII Project, Université Clermont-Auvergne, Clermont-Ferrand, France
[b] Centre d'Etudes et de Recherches sur le Développement International (CERDI), Université Clermont-Auvergne, Clermont-Ferrand, France
[c] International Material Flow Management Programme, Trier University of Applied Sciences, Environmental Campus Birkenfeld, Rheinland-Pfalz, Germany
[d] Institute for Sanitary Engineering, Water Quality, and Solid Waste Management and Technology (ISWA), University of Stuttgart, Stuttgart, Büsnau, Germany
[e] Federal Research Institute of Rio Grande do Sul, Bento Goncalves, Rio Grande do Sul, Brazil

ARTICLE INFO

Article history:
Received 13 January 2017
Received in revised form
10 July 2017
Accepted 17 July 2017
Available online 22 July 2017

Keywords:
Optical fiber
Life cycle impact assessment
MCVD
Carbon footprinting
Umberto

ABSTRACT

Optical fibers have become the backbone of long distance telecommunications, thus, reducing the environmental impacts of its production process poses as a crucial step towards its sustainable deployment worldwide. This paper presents and discusses the Life Cycle Impact Assessment of the Modified Chemical Vapor Deposition (MCVD) vitreous optical fiber production process. The environmental impacts of 18 production scenarios were analyzed and compared using the Umberto NXT modeling software, generating cradle-to-gate results in accordance to the criteria of two Project Oriented Environmental Management indicators: IPCC 2007 Global Warming Potential and ReCiPe Hierarchical Average Environmental Impact. Two main results were achieved: (a) the carbon footprint of the MCVD production process (8.02 $kgCO_2eq$ per kilometer of optical fiber, business as usual) – which represents a novel contribution to this field of scientific research –, and (b) less environmentally impactful production alternatives – namely metallic, ceramic and chalcogenic raw material combinations, renewable energies and a different catalyst. Secondary results and analyses of the production process were also discussed in order to highlight the importance of decision-making in raw material and energy sourcing strategies as drivers to reduce the environmental impacts of vitreous optical fiber production.

1. Introduction

Optical fibers were designed to surpass the current generation of copper- and aluminum-based communication technologies that permeate human relations (Schramm, 1988; Agrawal, 2003). They are already a key component in cloud computing, self-correcting networks, mobile data telephony and non-satellite wireless infrastructure (Artundo et al., 2011; CITEL, 2015).

According to the International Telecommunications Union (ITU), optical fibers' participation in overall telecommunications networks has grown significantly since 2013, especially in Europe (21.5%) and the Americas (14.2%) (ITU, 2010, 2015). Nevertheless, it is natural that all countries will seek the same reality of countries such as Japan and Korea, where optical connections have already exceeded 60% of the total (OECD, 2011; Hwang and Choi, 2012).

To ensure that optical communication systems are increasingly efficient, several experts and scientists are dedicated to the improvement of optical fibers' production processes, however, its environmental aspects are not yet thoroughly discussed (Bartnikas and Srivastava, 2003; Haykin, 2001).

There is an increasing number of laws, standards and certifications addressing environmental impacts in several areas – including telecommunications –, but few address optical fibers directly (Haykin, 2001; Mendez and Morse, 2007). Therefore, there is a gap not only in terms of legal and regulatory framework, but also scientific and technical studies regarding the environmental aspects of optical fibers (Deveau, 2001; Bartnikas and Srivastava, 2003).

This paper aims to contribute to the discussions within said gap

* Corresponding author. 36 Avenue Jean Jaurés, 63400, Chamalières, Auvergne, France.
E-mail address: julian.torres@live.it (J.T.M. Pinto).

http://dx.doi.org/10.1016/j.jclepro.2017.07.141
0959-6526/

and to suggest environmentally friendlier production arrangements and sourcing strategies. To that end, the physical and chemical data that permeate the environmental aspects of optical fiber production were surveyed, modelled and production scenarios were simulated.

1.1. The production process

Optical fibers weigh, on average, less than 1 g per meter and can be produced with ceramic (Farhi et al., 2009), polymeric (Carvalho, 2010; Ritzhaupt-Kleissl et al., 2006) and vitreous materials (Skorinkarpov et al., 2012; Mrabet et al., 2010), being the latter the most common for long range telecommunication (Bäumer, 2011; Poulain et al., 2003), especially when combined with rare-earth minerals such as erbium, ytterbium, gadolinium, praseodymium, and neodymium (Augustyn et al., 2011; Ballato et al., 2010; Churbanov et al., 2010).

Currently, the most common process to produce vitreous optical fibers is the modified chemical vapor deposition (MCVD) (Mendez and Morse, 2007), which consists of depositing several layers of SiO_2 and GeO_2 inside a glass tube that will undergo a stretching process (Agrawal, 2003; Ferdousi et al., 2012).

Fig. 1 shows the primary stage of the production process, which occurs in a precision lathe equipped with a hydrogen-oxygen transverse mobile blowtorch. The glass tube is placed in the lathe and, while it rotates, oxygen acts as a vehicle to inject $SiCl_4$ and $GeCl_4$ into it (Mendez and Morse, 2007). A gaseous catalyst is also injected to stabilize the temperature, namely phosphoric oxychloride ($POCl_3$, which breaks into P_2O_5) or boron tribromide (BBr_3, which breaks into B_2O_3) (Agrawal, 2003). As these gases are cyclically injected, the blowtorch moves along the tube, raising its temperature to 1500 °C. As a function of the temperature difference between the injected gases and the heated tube – a physical phenomenon known as thermophoresis (Prat et al., 2007) –, there is sequential deposition of thin layers of vapor on the inner walls of the silica tube, forming what will become the fiber's core (Bentzen, 2006; Lin et al., 2008; 2012).

Once all the layers have been deposited inside the silica tube, it goes through a sealing process, in which the torch reaches 2000 °C and runs the length of the tube until the high temperature causes the silica cladding to merge with the films deposited in its interior, configuring a solid cylinder known as preform. Next, the pulling/drawing is responsible for converting the preform into a fiber, a process that takes place in a mechanical system called a pulling/drawing tower, seen in Fig. 2.

The tower's feeding mechanism (V_1) inserts the preform into the center of a precision furnace (V_2), melting the preform at 2000 °C (2273.15 K) (Agrawal, 2003; Mendez and Morse, 2007). Based on the speed with which the preform is inserted into the furnace, its temperature, and the preform's viscosity, its own weight and the action of the force of gravity cause the material to stretch, creating a

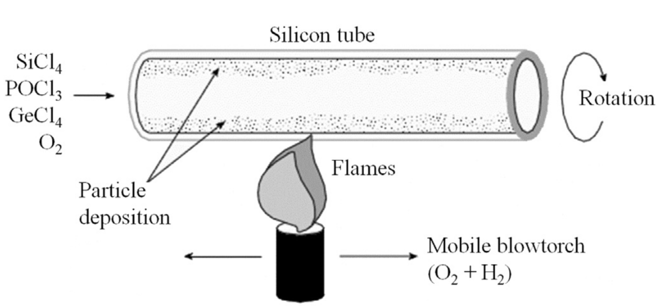

Fig. 1. Preform manufacturing process (adapted from Ribeiro, 2006).

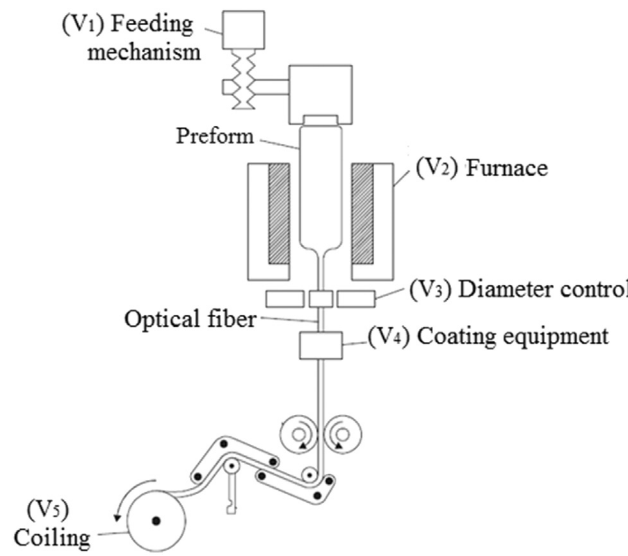

Fig. 2. Pulling/drawing process (adapted from ITU, 2010).

filament (Cheng and Jaluria, 2005; Lancry et al., 2012). At this temperature, the vitreous silica (SiO_2) rearranges its crystalline molecular angles and distances in order to become α-cristobalite, with a refractive index that can reach 2.34 (Vainshtein et al., 2000; Yang and Jaluria, 2009).

Shortly after leaving the furnace, the diameter of the filament is measured (V_3) and, as the fiber loses heat, it passes through an acrylate or silicone ultraviolet coating mechanism (V_4) (Agrawal, 2003). Finally, as a meter-long preform becomes a kilometers-long fiber, it is spooled onto a reel (V_5) (Ribeiro, 2006). Additional protective layers of coating can be then added to the fiber before it goes through performance and resistance testing (Achenie et al., 2006; Yang and Jaluria, 2009).

1.2. Environmental aspects

Just as any other material or product, optical fibers generate their own carbon footprint and specific environmentally hazardous emissions throughout the entire supply chain (Unger and Gough, 2007; Gutierrez et al., 2011).

According to Azapagic et al. (2004), changing how optical fibers are produced while keeping in mind factors such as transportation and reverse logistics can potentially reduce 30–60% of its current environmental impacts, depending on the end-of-life destination. Nevertheless, most studies about the environmental impacts of optical fibers focus on its operation, stage in which direct and indirect CO_2 emissions are present during installation (14%), use (77%), maintenance (1%) and end-of-life (8%) (Azapagic et al., 2004).

Few studies on optical fibers focus on the mineral extraction impacts of Silicon (Si) and especially of Germanium (Ge), both elements that have similar physical and chemical characteristics but that are distributed in the Earth's crust significantly differently and generate different types of environmental impacts as they are extracted:

Silicon in solid state is mainly surface-mined as silica quartz (SiO_2), and represents about 27–35% of Earth's crust, distributed in continental crusts (60.1%) and oceanic floors (39.9%) (Corathers, 2014; Dolley, 2015). Germanium, in turn, is present in Earth's crust at a rate of 1.5 mg/kg, and found mainly as a byproduct of deep-mining for Argirodite (Ag_8GeS_6) – with germanium content that ranges from 1.8 to 6.9% – and Germanite ($Cu_{13}Fe_2Ge_2S_{16}$) –

with germanium content between 5 and 10% (Bleiwas and Difrancesco, 2010; Guberman, 2015). Additionally, germanium in the form of Renierite, Briarite and Canfeldite can be found in the Earth's crust in concentrations ranging between 3 and 9% (Moskalyk, 2004; Guberman, 2015).

As a consequence, existing Life Cycle Analysis and Eco Design studies focused on optical fibers have shown that the most significant emissions to the atmosphere throughout an optical fiber's life span are CO_2, SO_2 and NO_2 (Shindell et al., 1998; Vondruska and Bednarik, 2009). In any case, even when the inherent impacts of their extraction are considered, the use of the aforementioned minerals generates less total emissions per kilometer to produce optical fibers than the emissions generated by the production of copper and aluminum cables for the same applications (Unger and Gough, 2007; Gutierrez et al., 2011).

Unfortunately, significant amounts of gaseous Chlorine (Cl_2) and gaseous Chlorine Dioxide (ClO_2) released during production have been left aside in the analyses conducted so far. These gases derive from the intensive oxidation of tetrachlorides during the thermophoretic stage of the production and can significantly increase the environmental impacts of the MCVD production process when released to the atmosphere (Azapagic et al., 2004). Both of these gases have high global warming potential when present in the troposphere (IPCC, 2007, 2013) and can substantially aggravate ozone layer depletion as Chlorofluorocarbons (CFCs) in the stratosphere (Kauffman, 1994; ISO, 2004, 2006, 2009).

At end-of-life, optical fibers can be sent to a landfill, incinerated, repurposed or recycled, being the latter the most environmentally friendly and preferred alternative from a legal perspective (Tietenberg, 2007; Twardowska et al., 2004). Significant progress has been made in the last 10 years on recycling the coating and structural materials that support vitreous optical fibers (Takahashi et al., 2004; Yokomizo et al., 2008), nevertheless, the most common destination is still incineration (Araujo et al., 2007) due to the lack of advanced recycling technologies that could efficiently turn the vitreous materials themselves into new optical cables, other vitreous materials (Giovannini and Kruglianskas, 2008; Parliament, 2015a; 2015b), or even solar panels (Bevis et al., 1983; DOE, 2001).

2. Methodology

The functional unit of this study is the MCVD production of 1 km of vitreous optical fiber. The objectives are to qualitatively and quantitatively explain, explore and discuss the environmental impacts of the functional unit using Life Cycle Impact Assessment, to test different productive scenarios within cradle-to-gate boundaries (Mcdonough and Braungart, 2002), to propose alternative raw materials and energy sources and to discuss sourcing strategies that can affect the overall environmental performance of the MCVD production process for vitreous optical fibers.

Within the boundaries are (a) the production processes of all involved materials and sources of energy, according to the demands of the vitreous optical fiber production process; (b) all processes concerning the manufacturing of the vitreous optical fiber itself, as described in section 1.1; and (c) the logistics within both the suppliers and the optical fiber manufacturer. It is important to note, however, that the transportation of the raw materials from the suppliers to the optical fiber manufacturer was considered performed by third-party transportation service providers, not posing as an environmental liability to either the optical fiber manufacturing company nor to the suppliers.

Based on the methodological steps taken throughout the study and depicted in Fig. 3, the methodology was divided in two parts. The first one focused on the production process itself and detailed the data used for calculating the variables that were used in the second part. The second part then described the parameters used for modeling the production process and the scenarios that enabled testing its different environmental impacts.

Throughout the study, priority was given to data acquired directly from industrial sources in the form of technical and operational reports. Lack of available data or lack of access to such data due to industrial privacy and non-disclosure policies led to the use of private and public databases or of data from state-of-the-art literature. In all cases, nevertheless, uncertainties were verified and minimized by directly parameterizing the model and the scenarios with physical and chemical calculations, better described in section 2.1.

2.1. Part one: producing 1 km of vitreous optical fiber

It is important to mention that all calculations presented in this section are based on the business as usual (BAU) scenario and were respectively adapted and parameterized into the model according to the stoichiometric, thermodynamic and raw material needs of each scenario. All scenarios are described in section 2.2.

The optical fiber considered for this study, detailed in Table 1, derives from those most commonly produced by the MCVD process and most commonly used for long distance telecommunications.

This study also considered (a) a 2 μm poly-methylmethacrylate (PMMA) coating layer generated by a UV curing process at 73% efficiency (Schmid and Toussaint, 2007; Döhler, 2003), (b) a 1 kg polypropylene precision cable reel for the coiling process (Yokomizo et al., 2008), (c) a glass tube delivered clean and unpacked directly into production, and (d) external oxygen supply derived 100% from cryogenic separation. The equations used during the study and the BAU stoichiometric balance of the production process are detailed in Tables 2 and 3, respectively.

In order to accurately define the raw material demand for producing 1 km of the optical fiber under study – seen in Table 4 –, it was important not only to consider the efficiency in the formation of SiO_2 and GeO_2 (Bentzen, 2006; Park et al., 2000), but also the fact that increasing temperatures hinders the breakdown and oxidation of $GeCl_4$ due to the generation of chlorine gas (Cl_2) (Walker et al., 2006; Yang et al., 2008). Accordingly, the presence and the

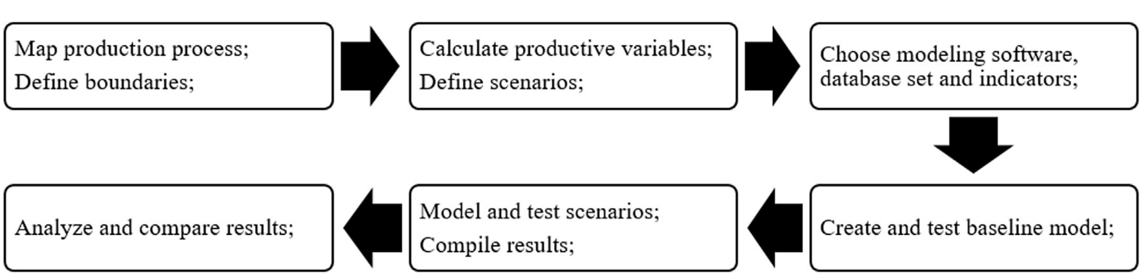

Fig. 3. Methodological steps.

Table 1
BAU physical and chemical characteristics of 1 km of the optical fiber under study.

Part	Substance	Presence (%)	Density (g/cm^3)	Mass per substance (g)	Chemical element	Composition (%)	Mass per element (g)	Total Volume (cm^3)
Core (Ø 8 μm)	SiO_2	82.30	2.1960	**9.08**	Si	46.74	**4.25**	**5.03**
					O	53.26	**4.84**	
	GeO_2	17.70	4.2500	**3.78**	Ge	69.42	**2.62**	
					O	30.58	**1.16**	
Cladding (Ø 129 μm)	SiO_2	90.00	2.1960	**2415.40**	Si	46.74	**1128.96**	**1222.12**
					O	53.26	**1286.44**	
	GeO_2	10.00	4.2500	**519.40**	Ge	69.42	**360.57**	
					O	30.58	**158.83**	
Coating (Ø 2 μm)	PMMA ($C_5H_9O_2$)	100.00	1.1800	**1.85**	C	59.41	**1.10**	**1.57**
					H	8.91	**0.16**	
					O	31.68	**0.59**	

Sources: Schmid and Toussaint (2007), Webelements (2015) and LANL (2015).

Table 2
Summary of equations.

	Name	Equation	Components
1	Volume of a straight cylinder	$V = \pi.R^2.h$	d specific heat c density G Gibbs' free energy
2	Mass of a solid body	$m = d.V$	G_p Product's free energy G_r Reagent's free energy
3	General equation of gaseous substances	$P.V = n.K.T$	H Enthalpy of formation h height
4	Heat demand, without phase change	$Q = m.c.\Delta T$	m mass n amount of moles P Pressure
5	Heat demand, during phase change	$Q = m.c$	Q Heat K General constant
6	Thermal energy	$\Delta G = \Delta H - T.\Delta S$	R Section S Entropy
7	Reaction energy	$\Delta G = Go - \Delta G_r$	T Temperature V Volume

Sources: Brady and Humiston (1986), Lide (2004).

concentration of the substances involved were calibrated.

For determining the energy demand of the production process, data was acquired from industrial technical and operational reports, from literature and from public databases (further detailed in section 2.2) and divided into thermodynamic demand and electricity demand. For the first, a chemical thermophoretic deposition efficiency of 29% was considered for particles smaller than 2.5 μm when the temperature difference between the glass tube and the gases injected to its interior does not surpass 1.65 K during preform fabrication (Weinberg, 1982; Greif and Joh, 1994; WEBB, 2012). As a consequence, the overall productivity observed was, on average, of 915 m/h, which represents an operation time of 1 h and 6 min to produce the intended 1 km of the optical fiber in study. Table 5 summarizes the thermodynamic data considered in the study.

Based on Table 5, the thermal energy demands to produce 1 km of optical fiber are shown in Table 6.

The thermodynamic demand of the production process was supplied by three different energy source combinations detailed in section 2.2. Nevertheless, electricity was also demanded by (a) a gas pump to heat the raw material gases and inject them at a flow between 7 and 8 L min^{-1}; (b) a UV coating system to cure 1.85 g of PMMA at 73% efficiency – resulting in 2.53 g of demand for this raw material –; and (c) a precision cable coiling/winding machine operating at 915 m/h. Table 7 shows the values considered for each of the aforementioned equipment – based on the average consumption of the three most common purchases for each equipment –, as well as the total electricity demand to manufacture 1 km of the optical fiber.

Table 3
BAU stoichiometric balance of the production process.

Raw material	Chemical reaction
$SiCl_4$	$SiCl_{4\ (25.69g)} + O_{2\ (4.84g)} \Delta\rightarrow SiO_{2\ (9.08g)} + 2Cl_{2\ (21.44g)}$
$GeCl_4$	$GeCl_{4\ (7.75g)} + O_{2\ (1.16g)} \Delta\rightarrow GeO_{2\ (3.78g)} + 2Cl_{2\ (5.13g)}$
$POCl_3$	$4POCl_{3\ (9.23g)} + 3O_{2\ (1.44g)} \Delta\rightarrow 2P_2O_{5\ (4.27g)} + 6Cl_{2\ (6.40g)}$

2.2. Part two: Life Cycle Impact Assessment

Umberto NXT modeling software (Umberto, 2015) was chosen to produce the Life Cycle Impact Assessment (Peças et al., 2013; Fthenakis et al., 2009), as well as to organize, calculate, analyze and compare how the involved materials and processes change their behavior as the variables of each scenario are introduced (Mcintosh et al., 2007; Matthews et al., 2011).

The chosen database set was Ecoinvent 3.01, which, at the time of this study, represented the largest available data source for environmental modeling purposes, consolidated and verified based on the International Reference Life Cycle Data System (ILCD) (Ecoinvent, 2015; Clear and Macdonell, 2011). To understand how the production process affects the environment – and not how the construction of the production facility itself does it –, each database was allocated sequentially as “Result” of the operation, and not as “Unit” of operation (Jakeman et al., 2006; Sonnemann et al., 2004). Priority was given to production patterns that represent worldwide business as usual practices, identified in Umberto NXT and in Ecoinvent as “GLO” (*Global*) or as the combination of country-specific practices with those from “RoW” (*Rest of the*

Table 4
BAU demand of raw materials for the production process.

Raw materials	Mass (g)	Liquid density (g/cm^3) [c]	Liquid volume (cm^3)	Gaseous volume (L) [d]
$SiCl_4$	88.57	1.50	59.05	75.85
$GeCl_4$	26.73	1.88	14.22	18.14
$POCl_3$ [e]	9.22	1.65	5.61	8.75
O_2 [a]	84.38	- [b]	- [b]	383.67
Total	**208.90**	-	**78.88**	**486.41**

[a] Oxygen is an indirect raw material, working as vehicle at a 50% ratio.
[b] Not applicable because it is present as gas.
[c] Sources: Fletcher et al. (2010) and Matweb (2015).
[d] At constant 1 atm pressure.
[e] $POCl_3$ is an indirect raw material, working as a catalyst to boost the oxidation of $SiCl_4$ and $GeCl_4$.

Table 5
BAU thermodynamic data of the substances present in the production process.

Reagents	Specific heat when liquid (J/K.mole)	Specific heat when gaseous (J/K.mole)	Boiling enthalpy (kJ/mole)	Boiling temperature (K)	Formation enthalpy (kJ/mole) [f]	Entropy (J/K.mole)
$SiCl_4$	145.30	90.30	28.70	330.80	−657.00	330.70
$GeCl_4$	165.30 [a]	96.10	27.90	359.70	−495.80	347.70
$POCl_3$	138.80	84.90	34.35	378.65	−558.50	324.20
O_2	- [b]	21.90	- [b]	- [b]	- [b]	- [b]
Products	**Specific heat when solid (J/K.mole)**	**Specific heat when liquid (J/K.mole)**	**Melting enthalpy (kJ/mole)**	**Melting temperature (K)**	**Formation enthalpy (kJ/mole)** [f]	**Entropy (J/K.mole)**
SiO_2	44.40	44.40 [c]	9.60	1933	−922.00	228.98
GeO_2	52.10	52.10 [c]	9.60 [d]	1388	−657.00	330.70
P_2O_5	- [b]	- [b]	- [b]	- [b]	−843.80 [e]	279.80 [e]

[a] Not yet chemically defined and unavailable in literature. Calculations considered average value between $SiCl_4$ and $SnCl_4$.
[b] Already gaseous, therefore not applicable.
[c] Not yet chemically defined and unavailable in literature. Calculations considered same value from solid phase.
[d] Not yet chemically defined and unavailable in literature. Calculations considered same value from SiO_2.
[e] Not yet chemically defined and unavailable in literature. Calculations considered same value as B_2O_3.
[f] Negative values represent exothermic reactions.
Sources: Prat et al. (2007), NIST (2015), Webelements (2015), Matweb (2015) and LANL (2015).

Table 6
BAU thermal-energetic balance of the production process.

Heating	**Energy to heat 1g (J/g)**	**Mass (g)**	**Subtotal (kJ)**
$SiCl_4$	963.45	88.57	85.34 [b]
$GeCl_4$	808.10	26.73	21.60 [b]
$POCl_3$	1069.03	9.22	9.86 [b]
O_2	1009.49	84.38	85.18
SiO_2	1089.97	2415.40	2632.71
GeO_2	734.40	519.40	381.45
Reacting	**Reaction energy (J/g)**	**Mass (g)**	**Subtotal (kJ)**
SiO_2	−1408.61 [a]	9.08	−12.80 [a]
GeO_2	−1252.45 [a]	3.78	−4.74 [a]
P_2O_5	−1439.06 [a]	4.27	−6.14 [a]
Melting	**Energy to melt 1g (J/g)**	**Mass (g)**	**Subtotal (kJ)**
SiO_2	1619.23 [b]	2424.49	3925.80 [b]
GeO_2	1075.09 [b]	523.18	562.47 [b]
Total			**7680.73**

[a] Negative values represent exothermic reactions.
[b] Includes phase changes.

World) (Tsai and Krogmann, 2012). Table 8 lists the databases used in the study in order to support and supplement data from industrial practices and from literature.

Two Project Oriented Environmental Management indicators (POEMs) were chosen. The first was IPCC 2007 Global Warming Potential (GWP) for 100 years – the most commonly used and so far, most consolidated method for carbon footprinting in kg of CO_2eq (Delucchi, 2003; Dbeis, 2016).

The second was ReCiPe Hierarchical Average (H.A.) Environmental Impact – which represents the updated and consolidated version of Eco-Indicator 99 and CML 2002, monitoring impacts as both source and sink in 17 natural sub-compartments, generating individual indicators known as midpoints; as well as in 3 categories that generate endpoint indicators: (a) ecosystem quality, (b) human health, and (c) resources availability (Nie et al., 2011; IES, 2010). Each of the 17 midpoint indicators and of the 3 endpoint indicators is calculated automatically by Umberto NXT based on the individual parameterizations created by Goedkoop et al. (2000, 2009) and regulated by the European Commission's Joint Research Center (JRC, 2010, 2013, 2014), respecting standards and criteria from key

Table 7
Electricity demand.

Production Stage	Process	Operation Time	Work Rate	Average Consumption	Total Consumption
Preform Fabrication	Injection	1 h 06min	7.37 L min^{-1}	1.38 W/min	**0.09 kWh**
Drawing	UV Coating	1 h 06min	915 m/h	400 W/h	**0.44 kWh**
Drawing	Coiling	1 h 06min	915 m/h	1 hp/h	**0.82 kWh**
Total					**1.35 kWh**

Sources: Eheim (2015), Lewa (2015), OCC (2015), Nordson (2015), Venrooy (2015) and Vetter (2015).

Table 8
Databases used in the study.

	Name	Scenarios
Energy	Heat production, natural gas, at industrial furnace >100 kW	All
	Heat production, at hard coal industrial furnace 1–10 MW	1,4,7,10,13,16
	Electricity production, hard coal	1,4,7,10,13,16
	Heat production, heavy fuel oil, at industrial furnace 1 MW	2,3,5,6,8,9,11,12,14,15,17,18
	Electricity production, oil	2,5,8,11,14,17
	Electricity production, geothermal	3,6,9,12,15,18
	Electricity production, wind, >3 MW turbine, onshore	3,6,9,12,15,18
	Heat and power co-generation, biogas, gas engine	3,6,9,12,15,18
Material	Polypropylene production, granulate	All
	Polymethyl methacrylate production, beads	All
	Silicon tetrachloride production	All
	Air separation, cryogenic	All
	Flat glass production, uncoated	All
	Phosphoryl chloride production	1 to 15
	Aluminum oxide production	4,5,6
	Refinery sulfur storage	10,11,12
	Selenium production	10,11,12
	Tin production	1 to 3, 16 to 18
	Chlorine production, liquid	1 to 3, 16 to 18
	Boric oxide production	16,17,18
	Copper oxide production	7,8,9
	Rare earth oxides production from bastnäsite concentrate	13,14,15

Source: Ecoinvent, 2015.

international agencies and institutions responsible for accounting and monitoring each type of environmental impact.

As is most common for MCVD manufacturing, all of the production processes were considered to be operated in enclosed and controlled laboratory environments, with constant atmospheric pressure and output gas collection – which enables the calculation of the direct gaseous Chlorine (Cl_2) and Chlorine Dioxide (ClO_2) emissions (Bartnikas and Srivastava, 2003; Mendez and Morse, 2007).

Table 9 summarizes the 18 scenarios created from three different energy source combinations (detailed in Table 10) and six different raw material combinations. The raw material combinations consist of completely replacing one of the raw materials with an alternative one, being those alternatives representative of the most recent and common studies in the field as of the time of this study itself:

- Metal doped substances (Al_2O_3 and Cu_2O) suggested as alternative raw materials by Neff et al. (2008) due to similar optical properties achieved with raw materials that are cheaper and easier to source than Germanium;
- Chalcogen doped substance (As_2S_3) suggested as alternative raw material by Churbanov et al. (2010) due to better optical properties achieved with raw materials that are more accessible worldwide than Germanium. Lack of Arsenic's chemical data was replaced with Selenium due to similar optical, bulk, shell,

Table 9
Scenarios.

Raw material combinations [a]	Catalyst and vehicle	Energy source combinations	Scenario number
$GeCl_4$	$POCl_3 + O_2$	Natural Gas + Coal	1 [b]
		Natural Gas + Oil	2
		Natural Gas + Oil + Renewable Mix	3
Al_2O_3 [c]	$POCl_3 + O_2$	Natural Gas + Coal	4
		Natural Gas + Oil	5
		Natural Gas + Oil + Renewable Mix	6
Cu_2O [c]	$POCl_3 + O_2$	Natural Gas + Coal	7
		Natural Gas + Oil	8
		Natural Gas + Oil + Renewable Mix	9
As_2S_3 [c]	$POCl_3 + O_2$	Natural Gas + Coal	10
		Natural Gas + Oil	11
		Natural Gas + Oil + Renewable Mix	12
$Pr_2O_3 + Nd_2O_3$ [d]	$POCl_3 + O_2$	Natural Gas + Coal	13
		Natural Gas + Oil	14
		Natural Gas + Oil + Renewable Mix	15
$GeCl_4$	$B_2O_3 + O_2$	Natural Gas + Coal	16
		Natural Gas + Oil	17
		Natural Gas + Oil + Renewable Mix	18

[a] All other raw materials ($SiCl_4$, glass tube, PMMA and cable reel) remained constant.
[b] Scenario 1 was chosen as the business as usual (BAU) scenario due to its representativeness among worldwide production practices.
[c] These substances require less thermodynamic energy to be broken and undergo thermophoresis (Edelstein, 2014), however, their reactions are proportionally less exothermic (NIST, 2015; LANL, 2015).
[d] These substances require more thermodynamic energy to release the Pr-1 and Nd-1 ions (Lide, 2004), however, their reactions are proportionally more exothermic (Bray, 2015; LANL, 2015).

ionization and electronic characteristics (George, 2015; Bedinger, 2015);
- Rare-earth substances (Pr_2O_3 and Nd_2O_3) suggested as alternative raw materials by Digonnet (2002) and Augustyn et al. (2011) due to better optical properties achieved with reduced productive issues, such as crystallization, when compared to Germanium. Both considered extracted at a 50% presence ratio from Bastnäsite mining (Samson et al., 2001; Gambogi, 2014);
- Alternative catalyst chosen due to its representativeness among worldwide productive practices and because breaking Boron Tribromide (BBr3) to form Boric Oxide (B_2O_3) has less exothermic catalysis potential but requires proportionally less heat to be broken (Crangle, 2015; Ober, 2015).

As seen above, many researchers have been attempting to replace Germanium in the optical fiber manufacturing process, motivated mainly by increasing sourcing costs due to direct or indirect unavailability. An additional challenge regarding Germanium is the absence of consistent midpoint and endpoint ILCD parameterization and normalization regarding its impacts towards metal depletion (Andrae and Vaija, 2017). In order to address this challenge, the present study adjusted the parameters and the normalization of Tin (Sn) – a database set available in EcoInvent 3.01 – to better represent Germanium based on (a) chemical and thermodynamic behavior similar to Selenium, Arsenic and Gallium (Höll et al., 2007; Anderson, 2014), as well as on (b) global metal depletion impacts derived from Germanium as a byproduct of Zinc, Copper, Silver and Arsenic extraction when present at 5.9% (Moskalyk, 2004; JRC, 2010, 2013, 2014).

The combinations of energy source shown in Table 8 were chosen based on the most common energy mixes that exist worldwide for industrial production of vitreous optical fiber (REN21, 2011; IEA, 2016) and are detailed in Table 10.

After modeling the production process and defining the databases, Umberto NXT software automatically replaced and rearranged the data on raw materials, catalysts, vehicles and energy sources for each scenario, generating results that were specific to each of them and that could be aggregated and compiled according to the desired analysis and discussion.

3. Results

Fig. 4 represents the model for the BAU scenario, in which it is possible to see the inputs (○) and outputs (○) of each production process. As the raw materials are brought together as intermediate outputs (○) by each of the manufacturing processes (□) within the preform manufacturing and drawing stages, more direct and indirect outputs were generated, all of which were considered in the results of the two chosen POEMs.

Presenting the model using Sankey diagrams allowed each arrow's colors to represent different types of environmental impacts that exist in the production process that originated it; the arrows' thicknesses, on the other hand, represent the scale of the environmental impact in relation to the product it generates. The model also generated inventory displacement data, which will be discussed in section 4.

After modeling each of the eighteen scenarios, the first main result was achieved by extracting the IPCC 2007 Global Warming Potential (GWP) indicators, in which different carbon footprint patterns were identified, as seen in Table 11. Special emphasis is given to the GWP of Scenario 1 (8.02 $kgCO_2eq$ per kilometer of optical fiber), for it is the first time it has been calculated for the production of vitreous optical fibers, in business as usual conditions.

With values that range from 6.36 to 8.75 $kgCO_2eq$ (a 37.58% difference) among the eighteen scenarios, it became clear how influential the decision-making in raw material and energy sourcing can be to the carbon footprint of the vitreous optical fiber production process.

The authors also used the IPCC 2007 Global Warming Potential (GWP) criteria to specifically analyze the emissions of gaseous Chlorine and Chlorine Dioxide released directly from the thermophoretic lathing process as a result of the oxidation of the raw materials that form the optical fiber's core, as seen in Table 12.

This secondary result also poses as a contribution to the gap found among the existing studies in this field, depicting how outputs of a single production process can substantially contribute to the rise in atmospheric temperatures worldwide if not properly managed.

Finally, the second main result derived from extracting the ReCiPe H.A. Total Environmental Impact indicators for the eighteen scenarios under study. A total of 306 midpoint indicators were generated – 17 different environmental sub-compartments for each of the 18 scenarios –, providing the final scores compiled in Table 13.

Table 10
Details of the energy source combinations.

Energy Source Combination	Participation per production process						Source	Capacity
	Heating	Injection	Lathing	Drawing	UV Coating	Coiling		
Natural Gas + Coal [a]	–	–	Heat (100%)	–	–	–	Direct Combustion	Up to 100 kW
	Heat (100%)	Electricity (100%)	–	Heat (100%)	Electricity (100%)	Electricity (100%)	Furnace Combustion	Up to 10 MW
Natural Gas + Oil [b]	–	–	Heat (100%)	–	–	–	Direct Combustion	Up to 100 kW
	Heat (100%)	Electricity (100%)	–	Heat (100%)	Electricity (100%)	Electricity (100%)	Furnace Combustion	Up to 1 MW
Natural Gas + Oil [b]	–	–	Heat (100%)	–	–	–	Direct Combustion	Up to 100 kW
	Heat (100%)	–	–	Heat (100%)	–	–	Furnace Combustion	Up to 1 MW
Wind + Geothermal [c]	–	Electricity (26.6%)	–	–	Electricity (26.6%)	Electricity (26.6%)	Wind Park Generation	Over 3 MW
Geothermal [c] + Biogas [d]	–	Electricity (4.9%)	–	–	Electricity (4.9%)	Electricity (4.9%)	Direct Generation	Up to 1 MW
	–	Electricity (68.5%)	–	–	Electricity (68.5%)	Electricity (68.5%)	Gas Engine	Up to 1 MW

[a] Electricity: Grid-connected Bituminous + Anthracite coal power plant, average global electrical efficiency of 32.2%. Heat: Fat egg coal industrial stoker boilers/furnaces, average global heating value of 28.9 MJ/kg.
[b] Electricity (grid-connected) and heat (local furnace): oil type S (European Quality) up to 500 MW capacity.
[c] Grid-connected Hot-Dry-Rock power plant with up to 1 MW capacity, operating with averages of binary-cycle (9%), backpressure (4%), single-flash (42%), double flash (21%) and dry-steam (24%).
[d] Grid-connected biowaste + sewage gas engine cogeneration plant, electricity efficiency 32%, heating value 22.73 MJ/Nm[c].
Sources: REN21 (2011), IEA (2016) and Ecoinvent (2015).

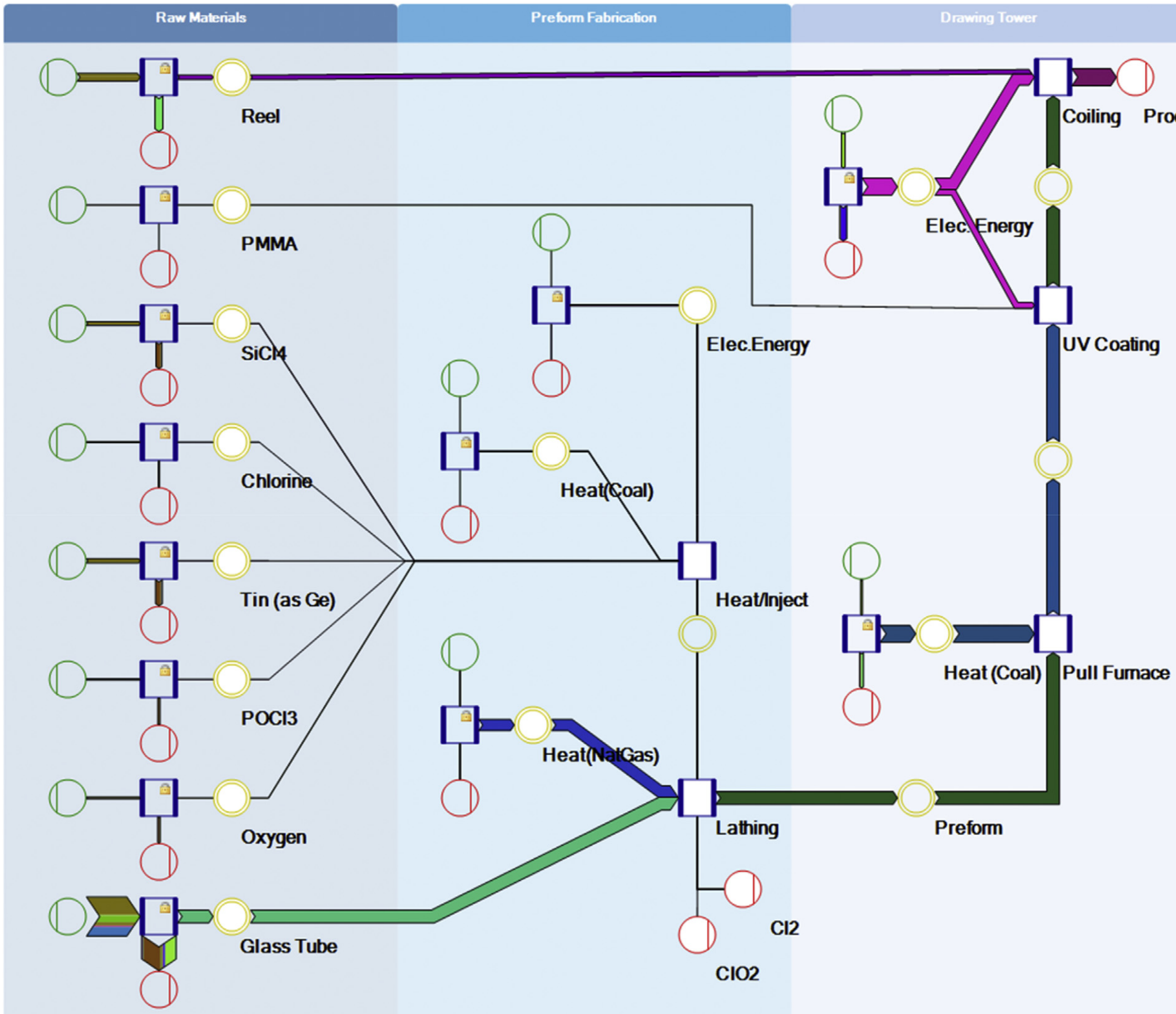

Fig. 4. Model for the BAU scenario, using Sankey diagram presentation.

Table 11
Summary of IPCC 2007 Global Warming Potential results and their shares per productive stage.

GWP	Natural Gas + Coal					Natural Gas + Oil					Natural Gas + Oil + Renewables				
Raw Material Variation	Scenario	kg CO_2eq	RawM (%)	PreF (%)	DraT (%)	Scenario	kg CO_2eq	RawM (%)	PreF (%)	DraT (%)	Scenario	kg CO_2eq	RawM (%)	PreF (%)	DraT (%)
BAU	1	8.02	69.91	4.17	25.93	2	7.53	74.54	4.08	21.38	3	6.56	85.55	3.68	10.76
Al_2O_3	4	7.83	69.16	4.27	26.57	5	7.33	73.87	4.18	21.95	6	6.36	85.11	3.80	11.09
Cu_2O	7	7.91	69.46	4.23	26.31	8	7.41	74.14	4.14	21.72	9	6.44	85.29	3.75	10.96
As_2S_3	10	7.84	69.21	4.26	26.53	11	7.34	73.91	4.18	21.91	12	6.38	85.14	3.79	11.07
Nd_2O_3+Pr_2O_3	13	8.75	72.39	3.82	23.79	14	8.25	76.77	3.72	19.51	15	7.28	86.99	3.32	9.70
B_2O_3	16	8.00	69.82	4.18	26.00	17	7.50	74.46	4.09	21.45	18	6.53	85.50	3.70	10.80

RawM = raw material extraction and production, including those for the purpose of energy generation.
PreF = preform fabrication.
DraT = drawing tower.

Once again, the results brought to light the importance of energy and raw material sourcing strategies in the production process, with results ranging from 0.77 to 1.55 points (a 101.30% difference). As seen in Table 11, using different raw materials and different sources of energy can significantly alter how this production process interacts with the environment both from the input and output perspectives.

4. Analyses, comparisons and discussions

4.1. Carbon footprint

The first set of analyses regards the first main result and is depicted by Fig. 5. The global warming potentials, when grouped by energy source combination, shows that using a mix of renewable

Table 12
Summary of the gaseous chlorine-based emissions for 1 km of optical fiber.

Substance	NFPA 704 [a]	Scenarios	Amount released (g)	Conversion Factor	IPCC 2007 GWP (kg CO_2eq) [c]
Chlorine (Cl_2)		1 to 3 and 16 to 18 4 to 15	183.23 147.87	1:8600 [b]	**1575.78** **1271.68**
Chlorine Dioxide (ClO_2)		1 to 3 and 16 to 18 4 to 15	12.80 10.33		**110.08** **88.84**

[a] Standard System for the Identification of the Hazards of Materials for Emergency Response.
[b] Conversion factor for CFC varieties based on UNDP (1987) and IPCC (2007).
[c] Considering 100% reactivity of the released amount to form CFC12 within 100 years.

Table 13
Summary of ReCiPe H.A. Total Environmental Impact indicators.

	Natural Gas + Coal					Natural Gas + Oil					Natural Gas + Oil + Renewables				
Raw Material Variation	Scenario	Total Points	RawM (%)	PreF (%)	DraT (%)	Scenario	Total Points	RawM (%)	PreF (%)	DraT (%)	Scenario	Total Points	RawM (%)	PreF (%)	DraT (%)
BAU	1	1.46	86.07	2.00	11.93	2	1.43	88.06	1.91	10.03	3	1.55	81.04	2.30	16.67
Al_2O_3	4	0.81	74.77	3.62	21.62	5	0.77	77.96	3.53	18.51	6	0.90	67.21	3.97	28.82
Cu_2O	7	0.95	78.53	3.08	18.40	8	0.92	81.36	2.98	15.65	9	1.04	71.66	3.43	24.90
As_2S_3	10	0.81	74.84	3.61	21.56	11	0.78	78.02	3.52	18.46	12	0.90	67.29	3.96	28.75
Nd_2O_3+Pr_2O_3	13	0.91	77.63	3.21	19.16	14	0.88	80.56	3.11	16.33	15	1.00	70.59	3.56	25.84
B_2O_3	16	1.46	86.04	2.00	11.96	17	1.43	88.04	1.92	10.05	18	1.55	81.00	2.30	16.70

RawM = raw material extraction and production, including those for the purpose of energy generation.
PreF = preform fabrication.
DraT = drawing tower.

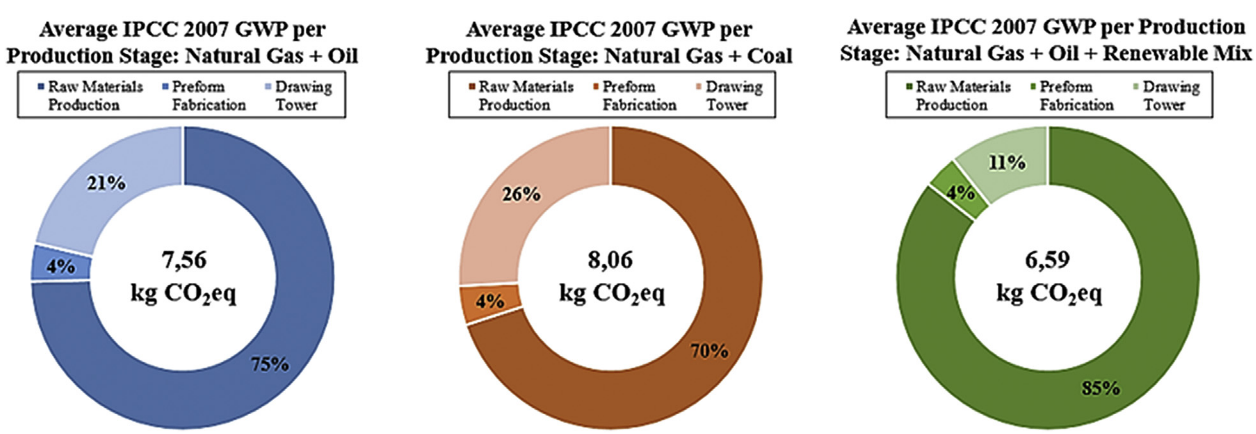

Fig. 5. Average global warming potential of each energy source, divided by production stage.

energies can be a less environmentally impactful alternative – 15.62% on average – for the production of vitreous optical fibers. Coal, on the other hand, would performed worse; a natural consequence of its emission intensive operation for generating heat and electricity, even increasing the share of the carbon footprint of the drawing tower.

Using renewable energies, however, significantly changes the share of environmental impacts throughout the cradle-to-gate approach on the production stages. Even though the total carbon footprint is reduced and drawing becomes proportionally less impactful due to the use of renewable energies, the resources necessary to produce this type of energy generate their own impacts earlier in the supply chain.

This shift in carbon footprint shares along the supply chain indicates the potential creation of energy sourcing strategies that transfer the liability or responsibility for the environmental impacts from the optical fiber manufacturer to the energy provider. Furthermore, reducing the overall footprint of the production process by employing renewable energies could favor the optical fiber manufacturer in matters of image and brand value based on environmentally friendlier behavior before its clients and society in general.

A new analysis emerges when addressing the carbon footprint from the perspective of the different raw material combinations that were tested. For each kilogram of final product, the raw material combinations with the least global warming potential are those derived from metallic- and chalcogen-based substances, as seen in Fig. 6.

Although the potential for reducing the carbon footprint seems marginal for a single kilogram of final product – varying between 1.63 and 2.75% –, its benefits could be remarkable when applied to industrial scale, as it is directly related to the scale of the

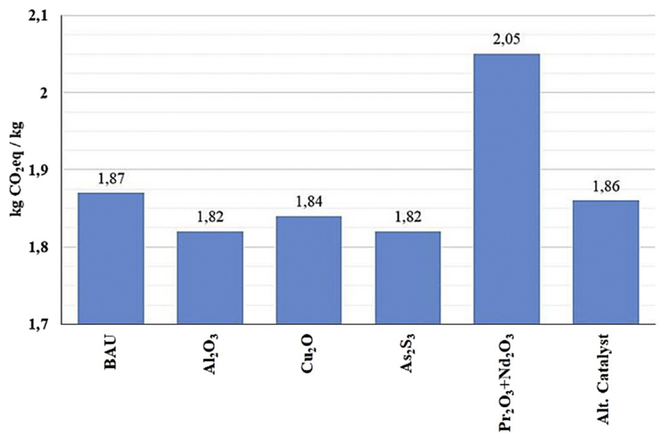

Fig. 6. kg of CO_2 equivalent emissions per kilogram of final product.

production. Given that fiber quality could range from similar to even better than business as usual, based on the studies that subsided the chosen scenarios, selecting a different raw material combination could not only pose as an additional sales argument – that of a cleaner product –, but also justify a substantial shift in operation and logistics, often capable of bringing along its own benefits regarding costs and efficiency.

With these results in mind, an optical fiber manufacturer could, for example, counterbalance a higher global warming potential derived from adopting a new raw material combination by increasing the participation of renewable energies in its energy sourcing strategies. Likewise, when renewable energy sources are unavailable, replacing a raw material with an alternative one capable of delivering same or similarly desirable results can balance the carbon footprint of the company's portfolio. Moreover, if properly amassed and treated, the chlorine-based emissions shown in Table 12 can be sold by the optical fiber manufacturer as a byproduct or serve as an input in other production processes, contributing to the company's circularity or recycling policies.

4.2. Environmental impacts

Focusing the analyses on the 306 midpoint indicators generated by the ReCiPe H.A. POEM helped deepen the discussion on raw material combinations. As summarized in Fig. 7, the scenarios that represent the most common practices nowadays (1 through 3 and 16 through 18) were the ones that scored highest in environmental impacts inflicted on the resources availability endpoint indicator. This was identified among the midpoint indicators as caused mainly by two factors: (a) metal depletion, responsible on average for 0.54 points; and (b) fossil fuel consumption, which represented 0.38 points on average. It is important to remind the reader, however, that the results of these scenarios reflect Germanium extracted as a byproduct at a presence of 5.9%, meaning that sourcing this metal from poorer ores in order to produce $GeCl_4$ would further increase its impacts on metal depletion and fossil fuel consumption.

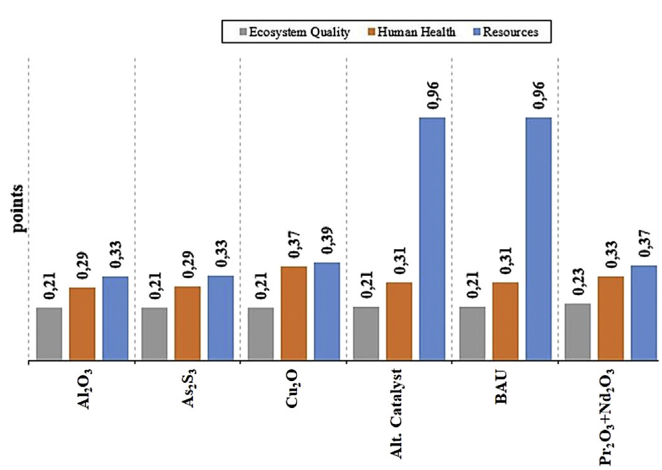

Fig. 7. ReCiPe H.A. endpoint indicators scores of different raw material combinations.

Analyzing the midpoint indicators for the metal doped and the chalcogen based scenarios (4–12) confirmed the better mineral extraction efficiency and productivity suggested by specific literature (Edelstein, 2014; Bray, 2015). Their relative abundance significantly lowered the impact on metals depletion and supported the arguments made by Neff et al. (2008) and Churbanov et al. (2010) about their affordability, but, in all cases, the fossil fuel consumption midpoint indicator remained high. These results suggest that raw material combinations based on metals and chalcogens could pose as more sustainable and affordable sourcing strategies from the perspective of the optical fiber manufacturer.

On the other hand, achieving the improved data transmission properties of producing optical fibers with the rare-earth raw material combinations (scenarios 13 through 15) – as suggested by Digonnet (2002) and Augustyn et al. (2011) –, even though slightly less harmful than the business as usual practices from the point of view of metals depletion, would still bring along a considerable increase in fossil fuel consumption as shown by the GWP analysis. As a consequence, decision-making that could reduce the environmental impacts by choosing these raw material combinations would heavily depend on costs, resource availability and logistics.

The impacts caused by different raw material combinations on the human health and on the ecosystem quality endpoint indicators, on the other hand, were subtler, more widely and more evenly distributed, summing up to 0.53 points on average. Ecosystem quality on all scenarios was mostly affected by the midpoint indicators of (a) climate change, ranging from 0.11 to 0.15 points; and (b) land occupation, ranging from 0.01 to 0.21 points. Human health on all scenarios was also mostly affected by (a) climate change, varying from 0.17 to 0.24 points; but also by the (b) formation of particulate matter, varying from 0.06 to 0.10 points. Based on these scores, an optical fiber manufacturer interested in reducing its overall environmental impacts could give preference to suppliers better capable of controlling their particulate matter emissions, as well as to those which are more efficient in their production – as in better equipped to extract the most raw materials from the least amount of land.

Fig. 8 further supports the discussion on the ReCiPe H.A. results, but approaches them from the energy source combinations' perspective. In it, it is possible to observe that using oil increased impacts on the resources availability endpoint indicator, a direct consequence of raw material production being an energy intensive stage of optical fiber manufacturing. Coal, on the other hand, was slightly more present in the drawing stage and even though it had lower impacts on resources availability than oil, its impacts on human health and ecosystem quality were higher. Analyzing the midpoint indicators further subsided these statements, linking coal to the highest scores on (a) formation of particulate matter and (b) human toxicity (both cancerous and non-cancerous, subject to case-by-case conditions).

Renewable energy sources, however, generated significantly different results. Although less impactful towards resources availability and human health, their impacts on ecosystem quality are substantially higher than what would usually be expected from a

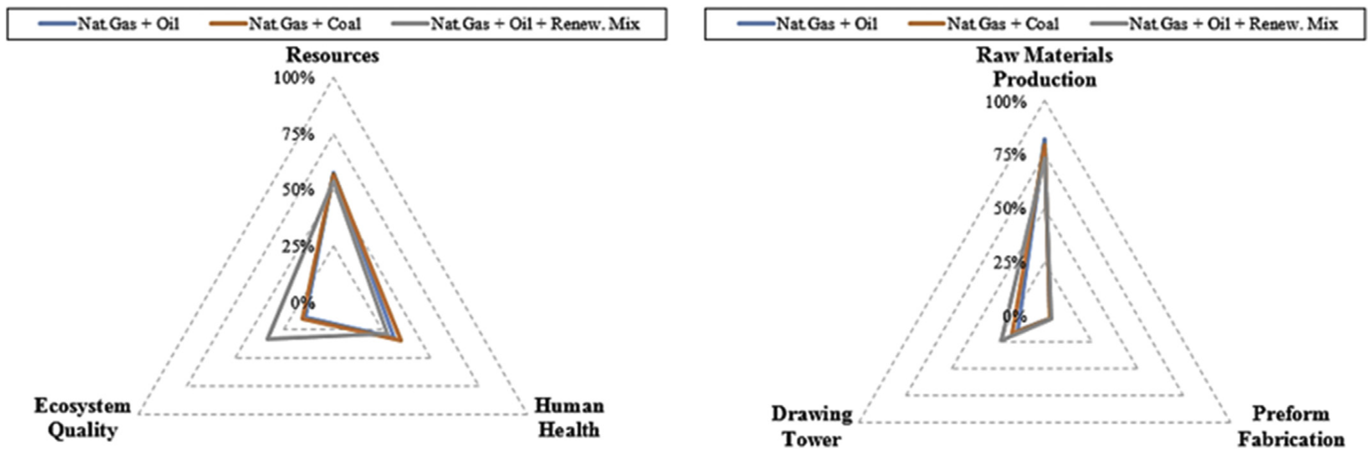

Fig. 8. ReCiPe H.A. endpoint indicators shares of different energy source combinations.

mix of supposedly cleaner alternatives. Nevertheless, delving into the midpoint indicators enabled understanding why the renewable energy mix contradicted such expectations, even when its potential for reducing the overall carbon footprint was verified: its worse environmental performance on terrestrial ecotoxicity and land occupation casted a substantial shadow over its advantages regarding fossil fuel depletion and climate change.

The terrestrial ecotoxicity midpoint indicator increased mostly due to the geothermal energy generation, which consists of injecting a fluid – usually water – onto underground heated rock beds. This fluid can be contained (or not) during and after injection. In non-contained systems, which rely on the geological structure itself, not on pipes, pressurized heated fluids can accelerate oxidation of substances present in the soil, as well as ease their dispersion at higher rates. Another factor that contributed to the results of this midpoint indicator was the existence of improper storage and disposal of the raw materials and the output sludge of biogas energy production, which often leads to soil contamination. With all said, however, a case-by-case approach would be required in order to subside decision-makers with actionable information about terrestrial ecotoxicity. Regarding land occupation, on the other hand, the highest impacts came from the amount of space necessary to build a wind park capable of generating the required electricity, as well as from the area necessary for the raw materials used in biogas generation to be created as byproduct of other agricultural activities.

Together, these two midpoint indicators drove up the ecosystem quality impacts of the studied renewable energy mix, pointing to the importance of carefully considering which types of renewable energy sources should be included or not in optical fiber production. Additionally, these results have shown that the inclusion of renewable energies into sourcing strategies with the single objective of reducing carbon footprints might inadvertently lead an optical fiber manufacturer to increase other environmental impacts. With this in mind, it would be beneficial for decision-making on renewable energy sources if the participation of each renewable source was rebalanced to minimize impacts, according to regional availability. Evaluating the environmental advantages and disadvantages of electricity generated by photovoltaic panels could also bring another alternative into the discussion, but such hypothesis was not tested in this study due to its current unrepresentative participation in optical fiber production.

4.3. Inventory displacement

Figs. 9 and 10 were created to compile the data acquired directly from the model regarding inventory displacement. They represent the final amounts of materials displaced between specific natural compartments – namely water, ground and air – in order to obtain the final product. Negative values classify compartments as sources, while positive values classify them as sinks. In the case of optical fiber production, the use of resources from water and ground

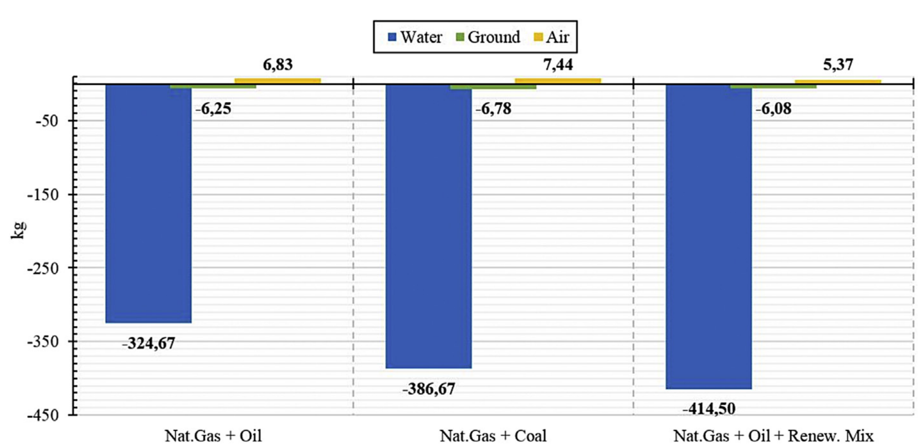

Fig. 9. Inventory displacement as a function of choosing different energy sources (in kg).

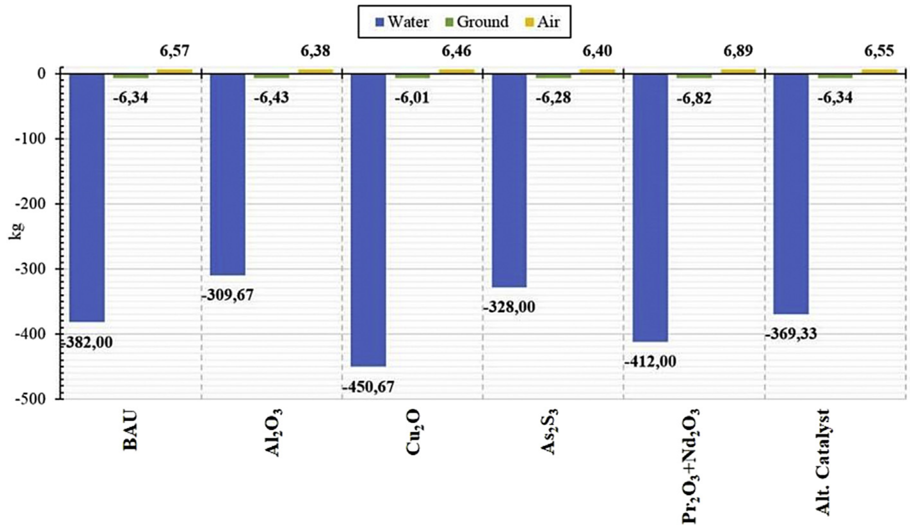

Fig. 10. Inventory displacement as a function of choosing different raw materials (in kg).

compartments is what allows the product to be manufactured, but results in emissions to the air compartment.

From the energy sourcing perspective, the adoption of the proposed renewable energy mix was responsible for the least amount of emissions to the atmosphere and was the one that used the least resources from the ground, however, its dependency on water was higher. These results were supported by the ReCiPe H.A. midpoint indicators, which pointed to geothermal and biogas energy sources as being the most water demanding. Coal and oil performed better regarding water consumption, but both at the expense of atmospheric emissions and ground resources.

This analysis allows an optical fiber manufacturer to better direct its energy sourcing strategies based on which compartments it would like to target for improvement. Manufacturers that have suppliers located in water scarce regions could opt for using energy from oil while mitigating the effects of the productive process on the atmosphere, for example. When water is abundant but air pollution is an issue, renewable energy sources would become more compelling. In any case, however, the carbon footprint and the environmental impacts previously discussed should be considered as well in order to ascertain that no other indirect impacts are being caused.

The same analysis was conducted for the different raw material combinations. As seen in Fig. 10 and supported by the ReCiPe H.A. midpoint indicators, choosing rare-earth substances demanded the most ground resources, however, they demanded less water than the production of Cu_2O, for example, due to differences in the mining process. The mining process also positioned Al_2O_3 and As_2S_3 among the least ground and water demanding raw materials, on average, reinforcing their potential as less environmentally impactful alternatives. Additionally, confirming the results from the global warming potential analysis, the most atmospheric emissions derived from the business as usual, alternative catalyst and rare-earth scenarios.

5. Conclusions and recommendations

Manufacturing optical fibers using the MCVD process is resource and energy intensive, thus this study's attempt to reduce its demands and its environmental impacts. Roughly put, the MCVD process requires converting resources extracted from ground and water natural compartments into the final product while generating atmospheric emissions. However, after modeling and testing scenarios of this production process, previously unexplored nuances capable of affecting decision-making were brought to light.

Fig. 11 represents the conclusions of the present study, ranking all scenarios in a dimensionless scale created merely to compile the results of both of the Project Oriented Environmental Management indicators. The scores in this scale range from 0 to 100 and derive from multiplying each scenario's ReCiPe H.A. Total Environmental Performance by their respective IPCC 2007 Global Warming Potentials.

In summary, this study has not only benchmarked the carbon footprint of the most commonly produced optical fiber at 8.02 $kgCO_2eq/km$, but also pointed to Al_2O_3, As_2S_3 and Cu_2O as interesting alternatives to $GeCl_4$ as raw materials due to their ability to provide similar and even better optical properties to the final product while also improving the overall environmental performance, especially when associated with the use of renewable energies. Pr_2O_3 and Nd_2O_3 also performed better in terms of environmental impacts when compared to business as usual practices, but the authors suggest that optical fiber manufacturers conduct a detailed economic analysis in order to ascertain that their costs would not be prohibitive, even when the superior optical properties of these substances are considered. Using B_2O_3 as the catalyst instead of $POCl_3$, on the other hand, would be the easiest change to make in the production process in order to reduce environmental impacts, however, the benefits would be marginal.

From the energy sourcing perspective, the carbon footprints demonstrated by the global warming potentials of the proposed renewable energy mix outperformed the coal and the oil alternatives, also making the drawing stage of the production proportionally less impactful. However, renewables did not always pose as the most favorable solution for environmental performance when other impacts were considered. Despite the growing representativeness of geothermal, wind and biogas as energy sources in worldwide industrial activities, their use in optical fiber production was responsible for increasing terrestrial ecotoxicity and land occupation, impacts which tend to manifest themselves in earlier steps of the supply chain.

Even though including renewable energy in sourcing strategies can be beneficial for an optical fiber manufacturer's carbon footprints, sales arguments and even brand value, decision-making in

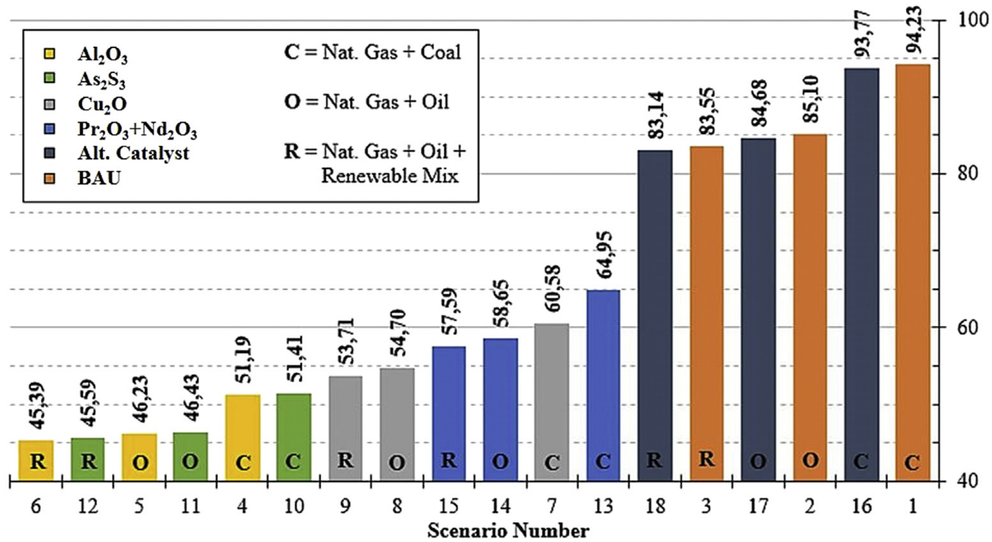

Fig. 11. Overall environmental impacts of the scenarios under study.

this matter should carefully consider (a) the regional availability of renewable sources as well as (b) the best mix to supply each productive process, thus avoiding unforeseen or unwanted collateral environmental impacts. Migrating from coal to oil energy sources would already improve environmental performance, but during the last couple of decades such transition has become less desirable from the environmental point of view than the use of renewables.

By analyzing the results of each scenario, it was possible to note that cradle-to-gate sourcing strategies are important drivers to reduce the environmental impacts of the MCVD production process. Decision-making in this matter, however, can substantially change the interactions of the optical fiber manufacturer with its suppliers. As discussed in section 4, choosing to produce optical fibers using different raw material combinations or different energy source combinations can have transferring, balancing and compensating effects while also shifting the relations of liability and responsibility for each environmental impact throughout the supply chain.

Considering that an optical fiber manufacturer has more agency over its decision-making process regarding the acquisition of energy and raw materials than regarding the efficiency with which they are produced, the authors suggest focusing on supplier development, aiming to identify and to favor the selection of suppliers capable of and interested in delivering energy and raw materials with better environmental performances themselves.

Future research in this field could test different raw materials suggested less extensively in the literature – such as those based on erbium, ytterbium, tellurium, niobium and bismuth (Manzani et al., 2016; Ni et al., 2016; Ragin et al., 2017; Nguyen et al., 2017) – as well as the impacts of other energy sources – namely photovoltaics, solar thermal, compressed air, heat exchange, nuclear and hydraulic. On the other hand, studies focused on the economic aspects, political influences or social impacts of optical fiber manufacturers' sourcing strategies would also pose as a substantial contribution towards decision-making aimed at sustainability in the telecommunications sector. Finally, the development of geochemical and mineralogical studies regarding Germanium's resource depletion potentials would be recommended in order to support further understanding of its environmental and economic impacts throughout optical fibers' and electronics' supply chains, especially when approached by LCIA.

References

Achenie, Luke E.K., Acquah, Charles, Datskov, Ivan, Mawardi, Andria's, Zhang, Feng, Pitchumani, Ranga, Santos, Eugene, 2006. Optimization of an optical fiber drawing process under uncertainty. Ind. Eng. Chem. Res. 45 (25), 8475–8483. http://dx.doi.org/10.1021/ie060045u.

Agrawal, Govind P., 2003. Fiber-optic Communication Systems, fourth ed. John Wiley & Sons, New Jersey, United States of America. ISBN 0-471-22114-7.

Andrae, Anders S.G., Vaija, Mikko S., 2017. The Life Cycle Assessments of an Optical Network Terminal and a Tablet: Experiences of the Product Environmental Footprint Methodology (Chapter 2). In: Advances in Environmental Research, vol. 55. Nova Publishers, New York, United States of America. ISBN 978-1-53610-904-7.

Anderson, C. Schuyler, 2014. 2014 Minerals Yearbook - Tin. United States Department of Interior: USGS Mineral Resources Program. Available at. https://minerals.usgs.gov/minerals/pubs/commodity/tin/index.html.

Araujo, Mishene C.P.B., Chaves, Arthur P., Espinosa, Denise C.R., Tenório, Jorge A.S., 2007. Electronic scraps – recovering of valuable materials from parallel wire cables. Waste Manag. J. 28 (11), 2177–2182. http://dx.doi.org/10.1016/j.wasman.2007.09.019.

Artundo, Iñigo, Tymecki, Andrzej, Ortego, Eduardo, Ortega, Beatriz, 2011. Cost forecasting of passive components for optical fiber network deployments. J. Opt. Fiber Technol. 17 (3), 218–226. http://dx.doi.org/10.1016/j.yofte.2011.02.001.

Augustyn, Elzbieta, Zelechower, Michal, Stroz, Danuta, Chraponski, Jacek, 2011. The microstructure of erbium–ytterbium co-doped oxyfluoride glass–ceramic optical fibers. J. Opt. Mater. 34 (6), 944–950. http://dx.doi.org/10.1016/j.optmat.2011.04.037.

Azapagic, Adisa, Wright, Elizabeth, Stevens, Gary, Mellor, Warren, Clift, Roland, 2004. Improving recyclability by design: a case study of fibre optic cable. Resources, Conserv. Recycl. J. 44 (1), 37–50. http://dx.doi.org/10.1016/j.resconrec.2004.09.005.

Ballato, J., Hawkins, T., Foy, P., Yazgan-Kokuoz, B., Mcmillen, C., Burka, L., Morris, S., Stolen, R., Rice, R., 2010. Advancements in semiconductor core optical fiber. J. Opt. Fiber Technol. 16 (6), 399–408. http://dx.doi.org/10.1016/j.yofte.2010.08.006.

Bartnikas, R., Srivastava, K.D., 2003. Power and Communication Cables - Theory and Applications. Wiley-IEEE Press, New Jersey, United States of America. ISBN 978-0-7803-1196-1.

Bäumer, S., 2011. Handbook of Plastic Optic, second ed. Wiley-VCH, New Jersey, United States of America. ISBN 978-3-527-63545-0.

Bedinger, George M., 2015. 2015 Minerals Yearbook - Arsenic. United States Department of Interior: USGS Mineral Resources Program. Available at. https://minerals.usgs.gov/minerals/pubs/commodity/arsenic/index.html.

Bentzen, Andreas, 2006. Phosphorus Diffusion and Gettering in Silicon Solar Cells. PhD Thesis. University of Oslo, Oslo, Norway.

Bevis, M., Irving, N., Allan, P., 1983. Recovery and re-use of polymeric cable scrap. Conserv. Recycl. J. 6 (2), 3–10.

Bleiwas, Donald I., Difrancesco, Carl, 2010. Historical Zinc Smelting in New Jersey, Pennsylvania, Virginia, West Virginia, and Washington, D.C., with Estimates of Atmospheric Zinc Emissions and Other Materials. United States Department of Interior, Reston, Virginia: USGS Open File Report.

Brady, James E., Humiston, Gerard E., 1986. General Chemistry – Principles and Structure. John Wiley & Sons, New Jersey, United States of America. ISBN 978-0-471-51784-9.

Bray, E. Lee, 2015. 2015 Minerals Yearbook - Aluminum. United States Department of Interior: USGS Mineral Resources Program. Available at. https://minerals.usgs.gov/minerals/pubs/commodity/aluminum/index.html.

Carvalho, M. de C., 2010. Redes de Bragg em Fibras Ópticas Poliméricas. PhD Thesis. Instituto Militar de Engenharia (IME), Rio de Janeiro, Brazil.

Cheng, Xu, Jaluria, Yogesh, 2005. Optimization of a thermal manufacturing process: drawing of optical fibers. Int. J. Heat Mass Transf. 48 (17), 3560–3573. http://dx.doi.org/10.1016/j.ijheatmasstransfer.2005.03.012.

Churbanov, M.F., Snopatin, G.E., Shiryaev, V.S., Plotnichenko, V.G., Dianov, E.M., 2010. Recent advances in preparation of high-purity glasses based on arsenic chalcogenides for fiber optics. J. Non-Crystall. Solids vol. 357 (11–13), 2352–2357. http://dx.doi.org/10.1016/j.jnoncrysol.2010.11.057.

CITEL – Interamerican Telecommunication Comission, 2015. Available at: https://www.citel.oas.org/en/Pages/Annual-Reports.aspx. Accessed on: 21 October 2015.

Clear, Tony, Macdonell, Stephen G., 2011. Understanding technology use in global virtual teams: research methodologies and methods. Inf. Softw. Technol. J. 53 (9), 994–1011. http://dx.doi.org/10.1016/j.infsof.2011.01.011.

Corathers, Lisa, 2014. 2014 Minerals Yearbook - Silicon. United States Department of Interior: USGS Mineral Resources Program. Available at. https://minerals.usgs.gov/minerals/pubs/commodity/silicon/index.html.

Crangle, J.R., 2015. 2015 Minerals Yearbook - Boron. United States Department of Interior: USGS Mineral Resources Program. Available at. https://minerals.usgs.gov/minerals/pubs/commodity/boron/index.html.

Dbeis, 2016. Government GHG Conversion Factors for Company Reporting. Department for Business, Energy & Industrial Strategy, London.

Delucchi, Mark A., 2003. A Lifecycle Emissions Model (LEM): Lifecycle Emissions from Transportation Fuels, Motor Vehicles, Transportation Modes, Electricity Use, Heating and Cooking Fuels, and Materials. Davis, California: Report of the Institute of Transportation Studies.

Deveau, Russell L., 2001. Fiber Optic Lighting: a Guide for Specifiers. ISBN 978-0-881-73325-9. Fairmont Press, New Jersey, United States of America.

Digonnet, Michel J.F., 2002. Rare-earth-doped Fibers, Lasers and Amplifiers: Revised and Expanded. Marcel Dekker, Stanford, United States of America. ISBN 978-0-824-70458-2.

DOE, 2001. Innovative Technology Summary Report: Copper Cable Recycling Technology. National Engineering and Environmental Laboratory, Idaho Falls, United States Department of Energy, Office of Environmental Management.

Döhler, Hardi, 2003. Improved Cure Speed and Efficiency of UV Curing Systems Using Silicone Acrylates. Tego Industrial Specialties, Essen, Germany.

Dolley, Thomas P., 2015. 2015 Minerals Yearbook - Silica. United States Department of Interior: USGS Mineral Resources Program. Available at. https://minerals.usgs.gov/minerals/pubs/commodity/silica/index.html.

Ecoinvent (2015). Swiss Center for Life Cycle Inventories. Switzerland. Available at: http://www.ecoinvent.org/database/Accessed on: 07 January 2015.

Edelstein, Daniel L., 2014. 2014 Minerals Yearbook - Copper. United States Department of Interior: USGS Mineral Resources Program. Available at. https://minerals.usgs.gov/minerals/pubs/commodity/copper/index.html.

Eheim GmbH, 2015. Available at: https://www.eheim.com/en_GB/products. (Accessed 5 January 2015).

Farhi, H., Belkahla, S., Lebbou, K., Dujardin, C., 2009. BGO fibers growth by μ-pulling down technique and study of light propagation. Phys. Procedia 2 (3), 819–825. http://dx.doi.org/10.1016/j.phpro.2009.11.030.

Ferdousi, Sifat, Nag, Avishek, Reaz, Abu Sayeem, Tornatore, Massimo, Mukhejee, Biswanath, 2012. Mixed-line-rate optical network design with wavebanding. J. Opt. Switch. Netw. 9 (4), 286–296. http://dx.doi.org/10.1016/j.osn.2012.04.003.

Fletcher, David F., Cheung, Catherine K.W., Barton, Geoffrey W., 2010. A computational fluid dynamics model for co-deposition of silica and germania in the MCVD process. J. Non-Crystall. Solids 356 (1), 24–31. http://dx.doi.org/10.1016/j.jnoncrysol.2009.09.025.

Fthenakis, Vasilis, Wang, Wenming, Kim, Hyung Chul, 2009. Life cycle inventory analysis of the production of metals used in photovoltaics. Renew. Sustain. Energy Rev. 13 (3), 493–517. http://dx.doi.org/10.1016/j.rser.2007.11.012.

Gambogi, Joseph, 2014. 2014 Minerals Yearbook - Rare Earths. United States Department of Interior: USGS Mineral Resources Program. Available at. https://minerals.usgs.gov/minerals/pubs/commodity/rare_earths/index.html.

George, Micheal W., 2015. Minerals Yearbook - Selenium and Tellurium. United States Department of Interior: USGS Mineral Resources Program, p. 2015. Available at. https://minerals.usgs.gov/minerals/pubs/commodity/selenium/index.html.

Giovannini, Fabrizio, Kruglianskas, Isak, 2008. Fatores Críticos de Sucesso para a Criação de um Processo Inovador Sustentável de Reciclagem: um Estudo de Caso. Rev. Adm. Contemp. 12 (4), 931–951.

Goedkoop, Mark, Effting, Suzanne, Collignon, Marcel, 2000. The Eco-indicator 99-A Damage Oriented Method for Life Cycle Impact Assessment: Manual for Designers. Amersfoort. Ministry of Housing, Spatial Planning and Environment (VROM), Netherlands.

Goedkoop, Mark, Heijungs, Reinout, Huijbregts, Mark, Schryver, An, Struijs, Jaap, Van Zelm, Rosalie, 2009. ReCiPe 2008-A Life Cycle Impact Assessment Method Which Comprises Harmonised Category Indicators at the Midpoint and the Endpoint Level. Centrum Milieukunde Leiden (CML), for the Dutch Ministry of Housing, Spatial Planning and Environment (VROM).

Greif, R., Joh, S., 1994. The effects of SiCl4 and GeCl4 oxidation, variable properties, buoyancy and tube rotation on the modified chemical vapor deposition process. Int. J. Heat Mass Transf. 38 (10), 1911–1921. http://dx.doi.org/10.1016/0017-9310(94)00238-Q.

Guberman, David, 2015. 2015 Minerals Yearbook - Germanium. United States Department of Interior: USGS Mineral Resources Program. Available at. https://minerals.usgs.gov/minerals/pubs/commodity/germanium/index.html.

Gutierrez, Jose, Riaz, Tahir, Pedersen, Jens M., Patel, Ahmed, Madsen, Ole B., 2011. Analytical model based on green criteria for optical backbone network interconnection. J. Comput. Stand. Interfaces 33 (6), 574–586. http://dx.doi.org/10.1016/j.csi.2011.03.005.

Haykin, Simon S., 2001. Communication Systems. John Wiley & Sons, New Jersey, United States of America. ISBN 978-0-471-17869-9.

Höll, R., Kling, M., Schroll, E., 2007. Metallogenesis of germanium - a review. Ore Geol. Rev. 30 (3–4), 145–180. http://dx.doi.org/10.1016/j.oregeorev.2005.07.034.

Hwang, J.K., Choi, T.I., 2012. A complex communication network for distribution automation using a fiber optic network and WLANs. J. Electr. Power Energy Syst. 43 (1), 812–817. http://dx.doi.org/10.1016/j.ijepes.2012.06.039.

IEA, 2016. Key World Energy Statistics. International Energy Agency, Paris, France.

IES, 2010. International Life Cycle Data System Handbook: Analysing of Existing Environmental Impact Assessment Methodologies for Use in Life Cycle Assessment. European Commission, Joint Research Centre, Institute for Environment and Sustainability, Luxembourg.

IPCC, 2007. Chapter 1: historical overview of climate change science. In: Climate Change 2007-Working Group I - the Physical Science Basis. Cambridge University Press, Cambridge.

IPCC, 2013. Climate Change 2013-The Physical Science Basis – Summary for Policymakers. Intergovernmental Panel on Climate Change, Geneva, Switzerland.

ISO, 2004. ISO 14001:2004: Environmental Management System – Requirements and Guiding for Use. International Organization for Standardization, Geneva, Switzerland.

ISO, 2006. ISO 14064:2006: Greenhouse Gases - Part 1: Specification with Guidance at the Organization Level for Quantification and Reporting of Greenhouse Gas Emissions and Removals. International Organization for Standardization, Geneva, Switzerland.

ISO, 2009. ISO 14044:2004: Environmental Management – Life Cycle Analysis – Requirement Ans Orientations. International Organization for Standardization, Geneva, Switzerland.

ITU, 2010. Handbook Manual: Optical Fibers, Cables and Systems. International Telecommunications Union, Geneva, Switzerland.

ITU, 2015. Data Explorer. International Telecommunications Union. Available at: http://www.itu.int/ITU-D/ict/statistics/explorer/index.html. (Accessed 31 October 2015).

Jakeman, Anthony J., Letcher, R.A., Norton, J.P., 2006. Ten Iterative Steps in Development and Evaluation of Environmental Models. Environ. Model. Softw. J. vol. 21 (5), 602–614. http://dx.doi.org/10.1016/j.envsoft.2006.01.004.

JRC, 2010. ILCD Handbook: Analysis of Existing Environmental Impact Assessment Methodologies for Use in Life Cycle Asessment. European Commission, Joint Research Centre, Luxembourg.

JRC, 2013. JRC Technical Notes: Characterisation Factors of the ILCD Recommended Life Cycle Impact Assessment Methods. European Commission, Joint Research Centre, Luxembourg.

JRC, 2014. JRC Technical Reports: Normalisation Method and Data for Environmental Footprints. European Commission, Joint Research Centre, Luxembourg.

Kauffman, Joanne, 1994. Global environmental politics: lessons from Montreal. Environ. Impact Assess. Rev. 14 (1), 3–9. http://dx.doi.org/10.1016/0195-9255(94)90039-6.

Lancry, Matthieu, Régnier, Elise, Poumellec, Bertrand, 2012. Fictive temperature in silica-based glasses and its application to optical fiber manufacturing. J. Prog. Mater. Sci. vol. 57 (1), 63–94. http://dx.doi.org/10.1016/j.pmatsci.2011.05.002.

LANL (2015). United States: Los Alamos National Laboratory. Available at: http://periodic.lanl.gov/index.shtml Accessed on: 19 August 2015.

LEWA Pumps and Systems (2015). Available at: http://www.lewa.com/en/applications/Accessed on: 05 January 2015.

Lide, David R., 2004. Handbook of Chemistry and Physics, 84^{th} edition. CRC Press, New York, United States of America. ISBN 978-0-849-30484-2.

Lin, Jyh-Shyan, Tsai, Chuen-Jinn, Tung, Kuo-Lung, Chiang, Hann-Chyuan, 2008. Thermophoretic particle deposition efficiency in turbulent tube flow. J. Chin. Inst. Chem. Eng. 39 (3), 281–285. http://dx.doi.org/10.1016/j.jcice.2008.01.001.

Lin, Wen-Tsann, Wang, Shen-Tsu, Li, Meng-Hua, Huang, Chiao-Tzu, 2012. Enhancement of process capability for strip force of tight sets of optical fiber using Taguchi's Quality Engineering. J. Opt. Fiber Technol. 18 (2), 101–107. http://dx.doi.org/10.1016/j.yofte.2012.01.002.

Manzani, Danilo, Gualberto, Tiago, Almeida, Juliana M.P., Montesso, Murilo, Mendonça, Cléber R., Rivera, Victor A.G., De Boni, Leonardo, Nalin, Marcelo, Ribeiro, Sidney J.L., 2016. Highly nonlinear Pb2P2O7-Nb2O5 glasses for optical fiber production. J. Non-Crystall. Solids 443 (1), 82–90. http://dx.doi.org/10.1016/j.jnoncrysol.2016.04.019.

Matthews, K.B., Rivington, M., Blackstock, K.L., Mcgrum, G., Buchan, K., Miller, D.G., 2011. Raising the bar - the challenges of evaluating the outcomes of environmental modeling and software. Environ. Model. Softw. J. 26 (3), 247–257. http://dx.doi.org/10.1016/j.envsoft.2010.03.031.

Matweb, 2015. Chemical Material's Details. Available at: http://www.matweb.com. (Accessed 17 August 2015).

Mcdonough, William, Braungart, Michael, 2002. Cradle to Cradle: Remaking the Way We Make Things. North Point Press, New York, United States of America. ISBN 978-0-865-47587-8.

Mcintosh, B.S., Seaton, R.A.F., Jeffrey, P., 2007. Tools to think with? Towards understanding the use of computer-based support tools in policy relevant research. Environ. Model. Softw. J. 22 (5), 640–648. http://dx.doi.org/10.1016/j.envsoft.2005.12.015.
Mendez, Alexis, Morse, T.F., 2007. Specialty Optical Fibers Handbook. Academic Press, London, United Kingdom. ISBN 978-0-12-369406-5.
Moskalyk, R.R., 2004. Review of germanium processing worldwide. Miner. Eng. J. 17 (3), 393–402. http://dx.doi.org/10.1016/j.mineng.2003.11.014.
Mrabet, Hichem, Dayoub, Iyad, Attia, Rabah, Hamouda, Walaa, 2010. Wavelength and beam launching effects on silica optical fiber in local area networks. J. Opt. Commun. 283 (21), 4234–4241. http://dx.doi.org/10.1016/j.optcom.2010.06.034.
Neff, Martin, Romano, Valerio, Lüthy, Willy, 2008. Metal-doped fibres for broadband emission: manufacturing with granulated oxides. J. Opt. Mater. 31 (2), 247–251. http://dx.doi.org/10.1016/j.optmat.2008.04.001.
Nguyen, Vinh Q., Drake, Gryphon, Villalobos, Guillermo, Gibson, Daniel, Bayya, Shyam, Kim, Woohong, Baker, Colin, Chin, Geoff, Kung, Frederic H., Kotov, Mikhail I., Busse, Lynda, Sanghera, Jasbinder S., 2017. Effect of aluminum and tellurium tetrachloride addition on the loss of arsenic selenide optical fiber. Opt. Mater. 64, 327–333. http://dx.doi.org/10.1016/j.optmat.2016.12.038.
Ni, Jiasheng, Peng, G.D., Wang, Chang, Luo, Yanhua, Xiao, Gui, Wei, Shuen, Liu, Han, Liu, Tiegen, 2016. Study on pump optimizing for Bi/Er co-doped optical fiber. Measurement 79, 160–163. http://dx.doi.org/10.1016/j.measurement.2015.10.003.
Nie, Zuo-Ren, Gao, Feng, Gong, Xian-Zheng, Wang, Zhi-Hong, Zuo, Tie-Yong, 2011. Recent progress and application of materials life cycle assessment in China. Prog. Nat. Sci. Mater. Int. 21 (1), 1–11. http://dx.doi.org/10.1016/S1002-0071(12)60016-1.
NIST, 2015. Standard Reference Database 69: Chemistry WebBook. Available at: http://webbook.nist.gov/chemistry. (Accessed 17 August 2015).
Nordson (2015). Available at: http://www.nordson.com/en/divisions/industrial-coating-systems/application-solutions/uv-curing Accessed on: 05 January 2015.
Ober, Joyce, 2015. 2015 Minerals Yearbook - Bromine. United States Department of Interior: USGS Mineral Resources Program. Available at. https://minerals.usgs.gov/minerals/pubs/commodity/bromine/index.html.
OCC – Optical Cable Corporation (2015). Available at: http://www.occfiber.com/products/fiber-optic-cable Accessed on: 05 January 2015.
OECD, 2011. Fibre Access - Network Developments in the OECD Area. Organisation for Economic Cooperation and Development, Paris, France.
Park, K.S., Choi, M., Chung, J.D., 2000. Unsteady heat and mass transfer on the codeposition of SiO2/GeO2 during the modified chemical vapor deposition process. Int. J. Heat Mass Transf. vol. 43 (17), 3209–3217. http://dx.doi.org/10.1016/S0017-9310(99)00352-X.
Parliament, European, 2015a. Directive 2002/96/EC of 27 January 2003 on waste electrical and electronic equipment (WEEE). Eur. Union Off. J. Eur. Union, 2003. Available at: http://eur-lex.europa.eu/legal-content/EN/TXT/?uri=CELEX%3A32002L0096. Accessed on: 19 November 2015.
Parliament, European, 2015b. Directive 2012/19/EU of 4 July 2012 on waste electrical and electronic equipment (WEEE). Eur. Union Off. J. Eur. Union, 2015. http://eur-lex.europa.eu/legal-content/EN/TXT/?uri=uriserv%3AOJ.L_.2012.197.01.0038.01.ENG.
Peças, P., Ribeiro, I., Henriques, E., 2013. A life cycle framework to support materials selection for Ecodesign: a case study on biodegradable polymers. Mater. Des. 51, 300–308. http://dx.doi.org/10.1016/j.matdes.2013.04.043.
Poulain, M., Gougeon, N., El Abdi, R., 2003. Mechanical reliability of silica optical fibers. J. Non-Crystall. Solids 316 (1), 125–130. http://dx.doi.org/10.1016/S0022-3093(02)01944-0.
Prat, Oliver P., Cloitre, Thierry, Aulombard, Roger-Louis, 2007. Thermal and mechanical properties of silicon tetrachloride (SiCl4) and germanium tetrachloride (GeCl4) in their vapor and liquid phases. Chem. Vap. Depos. J. 13 (5), 199–203. http://dx.doi.org/10.1002/cvde.200604242.
Ragin, Tomasz, Zmojda, Jacek, Kochanowicz, Marcin, Miluski, Piotr, Jelen, Piotr, Sitarz, Maciej, Dorosz, Dominik, 2017. Enhanced mid-infrared 2.7 μm luminescence in low hydroxide bismuth-germanate glass and optical fiber co-doped with Er3 +/Yb3 + ions. J. Non-Crystall. Solids 457, 169–174. http://dx.doi.org/10.1016/j.jnoncrysol.2016.12.001.
REN21, 2011. Renewables 2011 Global Status Report. United Nations Environmental Program (UNEP), Paris, France.
Ribeiro, José Antônio Justino, 2006. Comunicações Ópticas. Érica, Rio de Janeiro, Brazil. ISBN 978-8-571-94965-2.
Ritzhaupt-Kleissl, E., Boehm, J., Hausselt, J., 2006. Thermoplastic polymer nanocomposites for applications in optical devices. Mater. Sci. Eng. C 26 (5–7), 1067–1071. http://dx.doi.org/10.1016/j.msec.2006.02.004.
Samson, B.N., Tick, P.A., Borrelli, N.F., 2001. Efficient neodymium-doped glass-ceramic fiber, laser and amplifier. Opt. Lett. 26 (3), 145–147. http://dx.doi.org/10.1364/OL.26.000145.
Schmid, Steven, R., Toussaint, Anthony, F., 2007. Optical Fiber Coatings. Specialty Optical Fibers Handbook. http://dx.doi.org/10.1016/B978-012369406-5/50006-0.
Schramm, Wilbur, 1988. The Story of Human Communication. Haper Collins, New York, United States of America. ISBN 978-0-060-45799-0.
Shindell, Drew T., Rind, David, Lonergan, Patrick, 1998. Increased polar stratospheric ozone losses and delayed eventual recovery owing to increasing greenhouse-gas concentrations. Nature 392, 589–592. http://dx.doi.org/10.1038/33385.
Skorin-karpov, Nina, Fudek, Marija, Pardo, Ramon Aparicio, Mariño, Pablo Pavón, 2012. Wavelength assignment for reducing in-band crosstalk attack propagation in optical networks: ILP formulations and heuristic algorithms. Eur. J. Oper. Res. 222 (3), 418–429. http://dx.doi.org/10.1016/j.ejor.2012.05.022.
Sonnemann, G., Castells, F., Schumacher, M., 2004. Integrated Life-cycle and Risk Assessment for Industrial Processes. CRC Press, London, United Kingdom. ISBN 978-1-566-70644-5.
Takahashi, Hiroshi, Ma, Wenhui, Ogura, Masaru, Takeshi, Kobayashi, 2004. Preparation of solar grade silicon from optical fibers wastes with thermal plasmas. Sol. Energy Mater. Sol. Cells J. 81 (4), 477–483. http://dx.doi.org/10.1016/j.solmat.2003.12.001.
Tietenberg, T.H., 2007. Environmental Economics and Policy, fifth ed. Pearson Addison Wesley, Harlow, United Kingdom. ISBN 0321348907.
Tsai, Ching-Ling, Krogmann, Uta, 2012. Material flows and energy analysis of glass containers discarded in New Jersey, USA. J. Ind. Ecol. 17 (1), 129–142. http://dx.doi.org/10.1111/j.1530-9290.2012.00509.x.
Twardowska, Irena, Allen, Herbert E., Kettrup, Antonius A.F., Lacy, William J., 2004. Solid Waste: Assessment, Monitoring and Remediation. Gulf Professional Publishing, Elsevier eBook, Houston, United States of America. ISBN 978-0-080-54147-1.
Umberto, 2015. Life Cycle Assessment and Carbon Footprint Software. Available at: https://www.ifu.com/en/umberto/. (Accessed 17 August 2015).
UNDP, 1987. Montreal Protocol: on Substances that Deplete the Ozone Layer. United Nations Development Program, Geneva, Switzerland.
Unger, Nicole, Gough, Oliver, 2007. Life cycle considerations about optic fibre cable and copper cable systems: a case study. J. Clean. Prod. 16 (14), 1517–1525. http://dx.doi.org/10.1016/j.jclepro.2007.08.016.
Vainshtein, Boris K., Fridkin, Vladimir M., Indenbom, Vladimir L., 2000. Structure of Crystals - Modern Crystallography. Springer Verlag, New York, United States of America. ISBN 978-3-642-57254-8.
Venrooy (2015). Available at: http://www.venrooy.com/products Accessed on: 05 January 2015.
Vetter Kabel (2015). Available at: http://www.vetter-kabel.de/en/products/fibre-optic-cable-laying/Accessed on: 05 January 2015.
Vondruska, Milan, Bednarik, Vratislav, 2009. Diminishable/removable sources of greenhouse gases. Int. J. Glob. Environ. Issues 9 (1–2), 193–196. http://dx.doi.org/10.1504/IJGENVI.2009.022095.
Walker, K.L., Geyling, F.T., Nagel, S.R., 2006. Thermophoretic deposition of small particles in the modified chemical vapor deposition (MCVD) process. J. Am. Ceram. Soc. 63 (9–10), 552–558. http://dx.doi.org/10.1111/j.1151-2916.1980.tb10763.x.
WEBB, Andrew S., 2012. Novel Optical Fibre Manufacturing Techniques for Yb-doped High-power Fibre Lasers and Sensing Applications. PhD Thesis. University of Southampton, Southampton, England.
Webelements, 2015. Description of Chemical Elements and Compounds. Available at: http://www.webelements.com. (Accessed 17 August 2015).
Weinberg, M.C., 1982. Thermophoretic efficiency in modified chemical vapor deposition process. J. Am. Ceram. Soc. 65 (2), 81–87. http://dx.doi.org/10.1111/j.1151-2916.1982.tb10362.x.
Yang, Jing, Jaluria, Yogesh, 2009. Feasibility and optimization of the hollow optical fiber drawing process. Int. J. Heat Mass Transf. 52 (17–18), 4108–4116. http://dx.doi.org/10.1016/j.ijheatmasstransfer.2009.03.033.
Yang, Ruichang, Liu, Ruolei, Zhou, Tao, Zhao, Lei, 2008. Kinematic characteristics and thermophoretic deposition of inhalable particles in turbulent duct flow. Chin. J. Chem. Eng. 16 (2), 192–197. http://dx.doi.org/10.1016/S1004-9541(08)60061-0.
Yokomizo, Kenji, Konda, Eiji, Ozawa, Toshiaki, Watanabe, Yuichi, Ebisawa, Masaru, 2008. Development of the optical fiber cable for recycling. In: International Cable and Connectivity Symposium (IWCS).